

Anticorrosion of WO₃-Modified TiO₂ Thin Film Prepared by Peroxo Sol-Gel Method

Jia-Ying Wu, Yu-Wen Chen*

Department of Chemical and Materials Engineering, National Central University, Taiwan

Email: *ywchen@cc.ncu.edu.tw

How to cite this paper: Wu, J.-Y. and Chen, Y.-W. (2020) Anticorrosion of WO₃-Modified TiO₂ Thin Film Prepared by Peroxo Sol-Gel Method. *Modern Research in Catalysis*, 9, 35-46.

<https://doi.org/10.4236/mrc.2020.93003>

Received: July 10, 2020

Accepted: July 28, 2020

Published: July 31, 2020

Copyright © 2020 by author(s) and Scientific Research Publishing Inc.

This work is licensed under the Creative Commons Attribution International License (CC BY 4.0).

<http://creativecommons.org/licenses/by/4.0/>



Open Access

Abstract

The aim of this study was to develop a method to prepare WO₃-TiO₂ film which has high anticorrosion property when it was coated on type 304 stainless steel. A series of WO₃-modified TiO₂ sols were synthesized by peroxo-sol gel method using TiCl₄ and Na₂WO₄ as the starting materials. TiCl₄ was converted to Ti(OH)₄ gel. H₂O₂ and Na₂WO₄ were added in Ti(OH)₄ solution and heated at 95°C. The WO₃-TiO₂ sol was transparent, in neutral (pH~7) solution, stable suspension without surfactant, nano-crystallite and no annealing is needed after coating, and very stable for 2 years in stock. WO₃-TiO₂ sol was formed with anatase crystalline structure. These sols were characterized by XRD, TEM, and XPS. The sol was used to coat on stainless steel 304 by dip-coating. The WO₃-TiO₂ was anatase in structure as characterized by X-ray diffraction. There were no WO₃ XRD peaks in the WO₃-TiO₂ sols, indicating that WO₃ particles were very small, possibly incorporating into TiO₂ structure, providing the amount of WO₃ was very small. The TiO₂ particles were rhombus shape. WO₃-TiO₂ had smaller size area than pure TiO₂. The SEM results showed that the film coated on the glass substrate was very uniform. All films were nonporous and dense films. Its hardness reached 2 H after drying at 100°C, and reached 5 H after annealing at 400°C. The WO₃-TiO₂ film coated on 304 stainless steel had better anticorrosion capability than the unmodified TiO₂ film under UV light illumination. The optimum weight ratio of TiO₂: WO₃ was 100:4.

Keywords

Anticorrosion, Photocatalyst, Nanocoating, WO₃-TiO₂, Coating, Sol-Gel Method, Nanomaterial

1. Introduction

TiO₂ has been well-known to be the good material for anticorrosion [1]. Yuan

and Tsujikawa [2] coated TiO₂ onto type 304 stainless steel, and reported that TiO₂ could protect the inner substrate stainless steel. The similar effects were reported by Tatsuma *et al.* [3] under UV light and γ -ray irradiation. They reported a photoelectrochemical anticorrosion system about TiO₂-WO₃. This research revealed an energy storage system with a sufficient capacity, which using WO₃ as an electron storage pool to receive the photogenerated electrons from TiO₂ conduction band. This system can promise that it can be effective in the dark for a while [3]. Adding WO₃ into TiO₂ can promote the anticorrosion capability under visible light irradiation [4]-[15]. However, most of previous studies used powder form or sol in acidic solution [4] [14] [15] [16] [17]. The powder WO₃-TiO₂ cannot be used to coat on substrate. The acidic sol is difficult to handle and cannot coat on some substrates. In previous studies, one of the authors has developed a peroxo-sol gel method to prepare TiO₂ sol. It is very stable and transparent after coating on substrate. None of previous literature was reported on WO₃-TiO₂ sol prepared by peroxo-sol gel method.

The aim of this study was to develop a method to prepare WO₃-TiO₂ sol by peroxo sol-gel method. The WO₃-TiO₂ sol was 1) transparent, 2) in neutral (pH~7) solution, 3) stable suspension without surfactant, 4) nano-crystallite and no annealing is needed after coating, 5) very stable for 2 years in stock. We also tried to find the optimum doping amount of WO₃, and to investigate its effect on anticorrosion after coating on stainless steel type 304.

2. Experimental

2.1. Preparation of WO₃-Modified TiO₂ Sols

Na₂WO₄ was purchased from Aldrich. The detail procedure of preparing WO₃-modified TiO₂ sol is as follows. The preparation method was the same as synthesis of pure TiO₂ sol, as reported in the previous studies [18]. The only difference was that Na₂WO₄ and H₂O₂ were added in the heating step at 95°C for 6 h under magnetic stirring. 6 h later, the transparent light yellow WO₃-TiO₂ sol was obtained. The molar ratio of TiO₂: H₂O₂ was 1: 6 and the weight ratio of WO₃: TiO₂ was 0.5:100, 1:100, 2:100 and 4:100, respectively. Ti(OH)₄ and Na₂WO₄ were converted to WO₃-TiO₂ crystallites at 95°C in the presence of H₂O₂. It should be noted that there was no surfactant was added. The sol was very stable even after 2 years in stock.

2.2. Preparation of WO₃-TiO₂ Films

WO₃-TiO₂ films were prepared by dip-coating method using the as-prepared WO₃-TiO₂ sols. The substrate was type 304 stainless steel. The total coating surface area of the substrate was 40 cm². Before coating, the substrate was cleaned by neutral abrasives and distilled water for several times, and then dried in an oven at 50°C. The substrate was vertically soaked into the as-prepared sol for 2 min, then pull out with the constant speed of 60 cm/min for 6 times. The thickness of WO₃-TiO₂ films was kept around 120 nm. After coating, it was heated at

400 °C. The number in parentheses means the weight percentage of WO₃ in the sample (Figure 1).

2.3. Characterization

2.3.1. X-Ray Diffraction (XRD)

The sample was prepared by drying the WO₃-TiO₂ sol at 100 °C for 2 days to obtain the powder form. The sample was calcined at 400 °C for 2 h. The crystalline structure of the as-prepared WO₃-modified TiO₂ powder was performed using Simens D500 powder diffractometer using CuK_α radiation ($\lambda = 1.5405 \text{ \AA}$) at a voltage and current of 40 kV and 40 mA, respectively.

2.3.2. Scanning Electron Microscopy (SEM)

The morphology and thickness of films were observed by Hitachi-3000 with tungsten lamp at acceleration voltage of 10 kV and emission current of 81,000 nA. The SEM sample was prepared by cutting the coated glass substrate into 0.5 cm × 0.5 cm piece with a diamond knife first and then coated with platinum to increase its conductivity.

2.3.3. Transmission Electron Microscopy (TEM)

The morphology and structure of WO₃-TiO₂ sol were observed by TEM (JEM-2000 EX II) operated at 160 kV or 200 kV. The TEM sample was prepared by dipping the carbon-coated copper grid (200 meshes) (Ted Pella) into as-prepared sol for 3 times.

2.4. Anticorrosion Test

The following methods were used to investigate the effect of WO₃-TiO₂ coating on anticorrosion capability of stainless steel 304.

2.4.1. The State of Corrosion

One of the methods to examine the state of the metal substrate is to place the coated substrate in a 3 - 5 wt% aqueous sodium chloride (NaCl) solution to carry

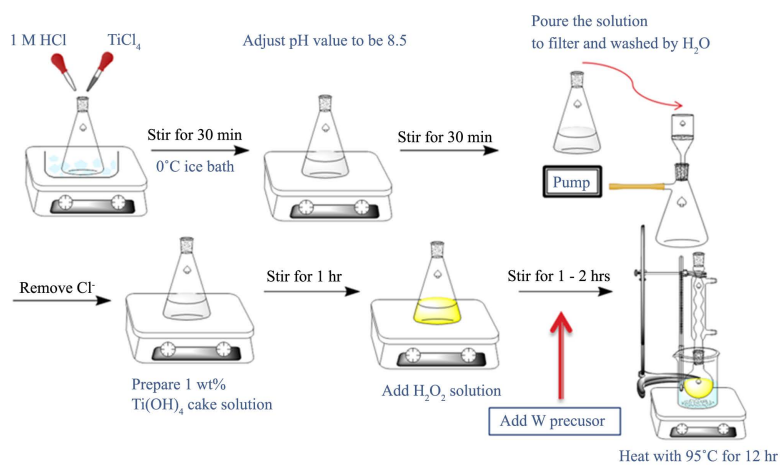


Figure 1. The procedure of preparing WO₃-TiO₂ sol.

out the salt spray test which is based on ASTM B-17. To speed the test, 5 wt% sulfuric acid aqueous solutions was used in this study. The state of the coated substrates was examined every 2 h. The weight of the substrates was measured every test and the corrosion degree ($\text{mg}/\text{dm}^2 \cdot \text{day}$) and erodibility (mm/year) were calculated.

$$\text{Corrosion degree}(\text{mg}/\text{dm}^2 \cdot \text{day}) = \frac{\Delta W}{S \times H} \times 24 \times 10^5 \quad (1)$$

$$\text{Erodibility}(\text{mm}/\text{year}) = \frac{W_1 - W_2}{d \times S} \times \frac{365 \times 24}{H} \times 10 = \frac{\Delta W}{d \times S \times H} \times 87600 \quad (2)$$

where W_1 is the weight before soaking into acidic solution (before testing) (g), W_2 is the weight after soaking into acidic solution (after rusting) (g), ΔW is the difference between W_1 and W_2 (g), d is density (g/cm^3), S is surface area (cm^2), and H is testing time (h).

2.4.2. Four-Point Probe

Four-point probe is the most commonly used instrument to measure the sheet resistance. As long as adding constant current into two probes, simultaneously measuring the voltage difference between the two probes, and the sheet resistance can be calculated.

The resistivity and sheet resistance were calculated by the following equation:

$$R = \frac{\rho}{t} \frac{l}{w} = R_s \frac{l}{w} \quad (3)$$

where R is resistance values (Ω), ρ is resistivity ($\Omega\text{-cm}$), l is the length of specimen (cm), w is the width of specimen (cm), t is the thickness of specimen (cm), and R_s is sheet resistance ($\Omega/\text{unit area}$).

2.4.3. Cyclic Voltammeter

The cyclic voltammeter is an instrument that can control the potential, and it can detect the current of electrochemical reaction. In the beginning, the electrode was washed by ultrapure water. The electrode was put in a beaker which contained 5 wt% NaCl solution. The OCP (Open Circuit Potential) was tested firstly and then the scanning potential range was set from -0.8 V to 0.6 V. The scanning rate of set potential was 0.05 V/s, and the scanning circles were 9. The method to analyze the effect of anticorrosion is electric polarization curve. The upper curve is anodic polarization and the lower one is the cathodic polarization curve. The anodic polarization curve represents the reduction of hydrogen during the whole experiment, *i.e.*, $2\text{H}^+ + 2\text{e}^- \rightarrow \text{H}_2$. The cathodic polarization curve shows the oxidation of metal, *i.e.*, $\text{M} \rightarrow \text{Mn}^+ + \text{ne}^-$. E_{corr} represents the potential that working electrode starts corrosion. The I_{corr} represents the corrosion current, which is the corrosion rate.

3. Results and Discussion

3.1. Characteristics of $\text{WO}_3\text{-TiO}_2$ Sols

$\text{WO}_3\text{-TiO}_2$ sol was light yellow transparent sol containing $\text{WO}_3\text{-TiO}_2$ nanoparticles dispersed in water. The yellow color was due to the presence of small

amount of titanium peroxide [18]. If one decreased the amount of H_2O_2 in preparation, the color became light yellow. The pH values of TiO_2 and $\text{WO}_3\text{-TiO}_2$ sols are listed in **Table 1**. The pH value of TiO_2 sol was 8.7. Adding WO_3 in TiO_2 sol decreased the pH value very slightly because the tungsten precursor was acidic and its amount was very low.

3.2. XRD

The XRD patterns of all the samples are shown in **Figure 3**. The result in **Figure 3** represents the anatase TiO_2 diffraction peaks located at $2\theta = 25.4102^\circ$, 37.9658° , 48.1227° , 62.7199° , and 75.2245° corresponding to the anatase phase of (101), (004), (200), (204), and (215). The as-prepared TiO_2 had low intensity peaks for anatase, as shown in **Figure 2(b)**, because the TiO_2 crystallites were very small, in agreement with literature data [14] [15] [16] [17] [18]. **Figure 3** shows the XRD patterns of $\text{WO}_3\text{-TiO}_2$ samples. The diffraction peaks of these patterns coincide with the characteristic peaks of anatase TiO_2 and did not match any diffraction peak of WO_3 . This is because the amount of WO_3 in $\text{WO}_3\text{-TiO}_2$ sample was very small. The characteristic peaks of $\text{WO}_3 \cdot \text{H}_2\text{O}$ are at $2\theta = 25.7164^\circ$, 35.1076° , and 52.7672° . In order to check whether the diffraction peaks of WO_3 appeared in W-TiO_2 samples or not, we added more amount of W precursors in the sample. **Figure 5** shows the XRD pattern of 1 wt% WO_3 -modified TiO_2 using H_2WO_4 as the precursor. There were no WO_3 XRD peaks in **Figure 5**. Tatsuma *et al.* [3] reported that WO_3 was highly dispersed in the bulk phase of TiO_2 particles and a new solid such as WO_3 was not formed. Our results are in accord.

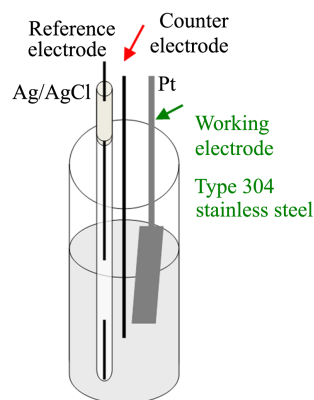


Figure 2. The schematic diagram of cyclic voltammeter.

Table 1. The pH values of the as-prepared sols.

Sample	pH value
TiO_2	8.78
WT (0.5)	8.78
WT (1)	8.68
WT (2)	8.43
WT (4)	8.32

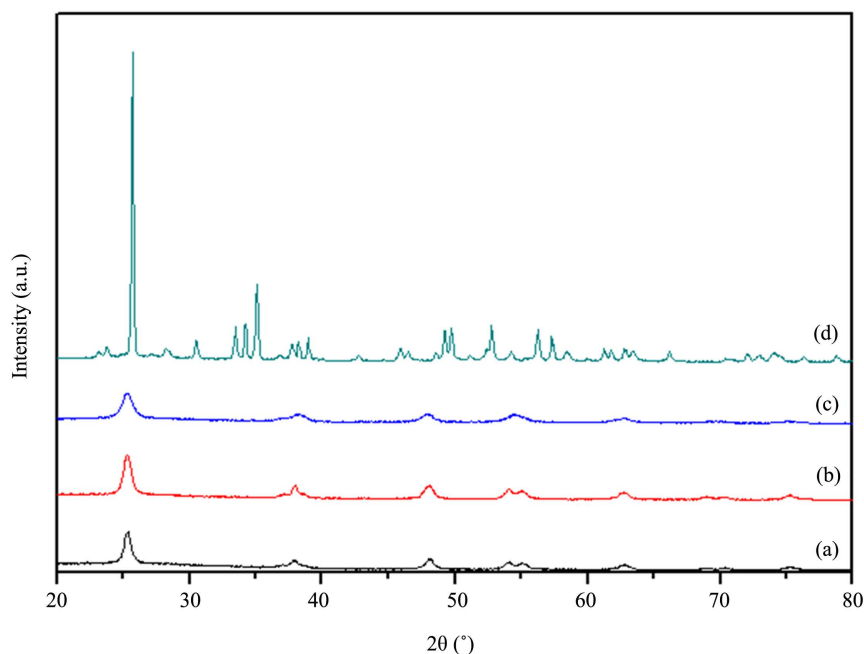


Figure 3. XRD patterns of (a) TiO_2 ; (b) WT (10); (c) WT (100); and (d) WO_3 .

3.3. SEM

The structure of TiO_2 and $\text{WO}_3\text{-TiO}_2$ films were examined by SEM. The top-view surface structure and cross-section view of the as-prepared thin film are shown in **Figure 4**. Each sample had very uniform and smooth surface of film on the top of substrate, indicating that dip coating is a good way to prepare the thin film. The surface of TiO_2 film was smoother than those of $\text{WO}_3\text{-TiO}_2$ samples. All films were nonporous and dense films. Its hardness reached 2 H after drying at 100°C , and reached 5 H after annealing at 400°C .

3.4. TEM

The morphology of as-prepared $\text{WO}_3\text{-TiO}_2$ sols was analyzed by TEM and HRTEM. HRTEM image in **Figure 5(a)** shows that the TiO_2 particles were rhombus shape with the major axis and minor axis of 30 - 50 nm and 15 - 30 nm, respectively. **Figure 5** also shows the morphology and particle size of the as-prepared $\text{WO}_3\text{-TiO}_2$. Comparing with pure TiO_2 sol, the particle sizes of $\text{WO}_3\text{-TiO}_2$ was smaller than that of TiO_2 . It is in agreement with the literature data reported by Tryba *et al.* [19]. No WO_3 particles were observed and one can conclude that W atoms were incorporated into the structure of TiO_2 , providing that the concentration of W precursor was low. In conclusion, we have successfully developed a method to prepare $\text{WO}_3\text{-TiO}_2$ sample.

3.5. Anticorrosion Test

The samples were loaded in the 5 wt% sulfuric acid solution to test their anti-corrosion capabilities. The results are shown in **Table 2** and **Table 3**. **Table 2** shows the results tested for 24 h and **Table 3** shows the results tested for 48 h.

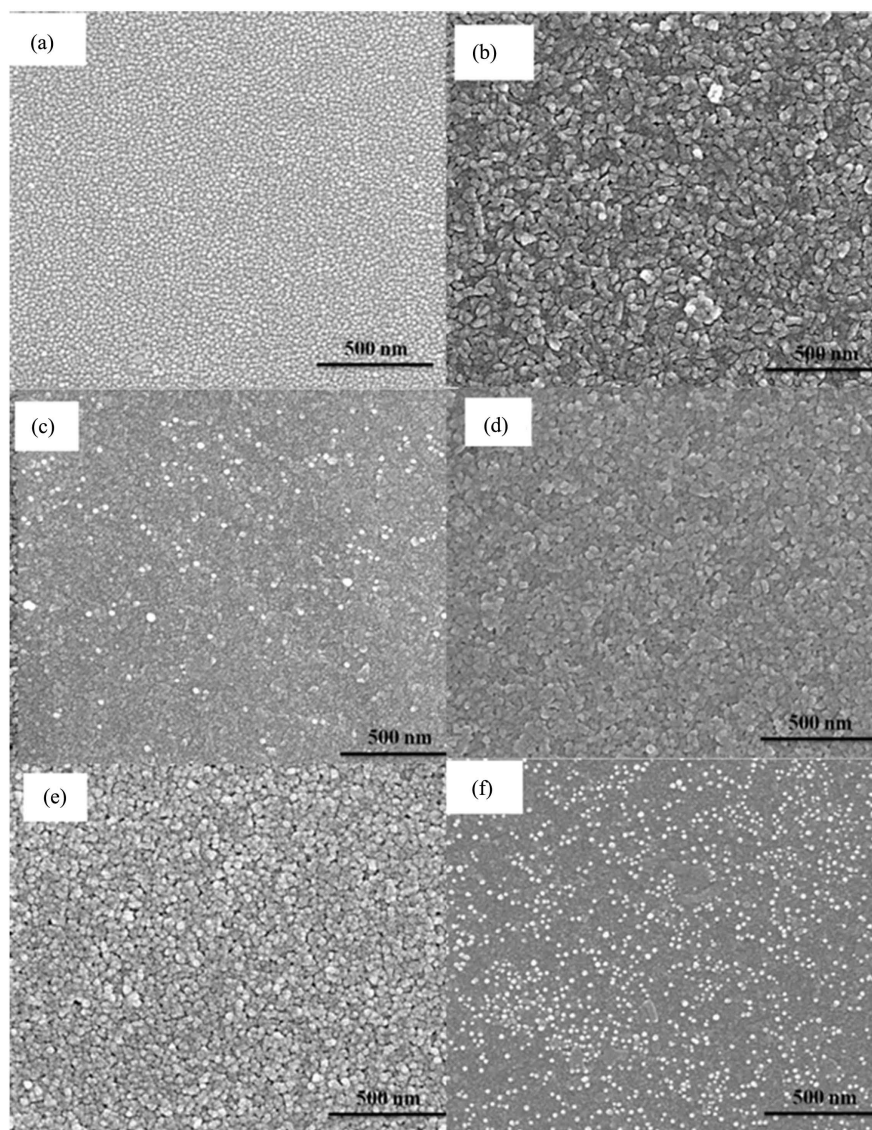


Figure 4. Top-view SEM images of the surface structure of (a) TiO₂ film; (b) WT (0.5) film; (c) WT (1) film; (d) WT (2) film; (e) HT (10) film and (f) HT (100) film.

Table 2. Weight loss of various samples in the 5 wt% sulfuric acid solution after 24 h.

Coating	weight before test (g)	weight after test (g)	Rate of corrosion $\times 10^5$ (g/cm ² ·min)
Bare substrate	9.0930	6.9609	12.339
TiO ₂	9.0989	7.4859	9.334
WT (0.5)	9.0942	7.5393	8.998
WT (1)	9.0778	7.5759	8.692
WT (2)	9.0733	7.4347	9.483
WT (4)	9.0635	7.4322	9.440
WO ₃	9.1027	7.3400	10.201

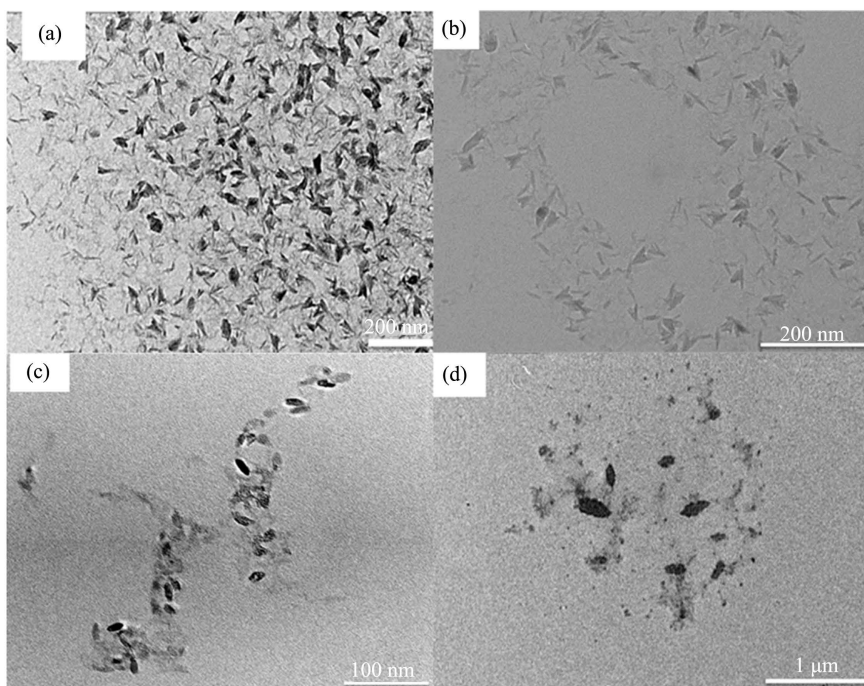


Figure 5. TEM image of (a) TiO_2 ; (b) WT (4) sol; (c) WT (10) sol and (d) WO_3 sol.

Table 3. Weight loss of the sample in 5 wt% sulfuric acid solution after 48 h.

Sample	weight before test (g)	weight after test (g)	rate of corrosion $\times 10^{-5}$ (g/cm ² ·min)
Bare substrate	9.0975	5.7162	19.57
TiO_2	9.0945	6.3181	16.07
WT (0.5)	9.0990	6.2845	16.29
WT (1)	9.0504	6.3375	15.70
WT (2)	9.0725	6.2969	16.06
WT (4)	9.0458	6.3673	15.50
WO_3	9.0741	6.2388	16.41

The bare sample without coating had very low resistance to corrosion. One can see in **Table 2** that sample WT (1) had the lowest weight loss by corrosion, indicating that it had the best anticorrosion performance among all the samples. Instead, WO_3 sample had low anticorrosion capability. **Table 2** and **Table 3** also show that the weight losses of all the samples coated with WO_3 - TiO_2 films were almost the same. The difference was small because the short time test was used. The results indicated that TiO_2 has good anticorrosion property. Adding suitable amount of WO_3 in TiO_2 improved the anticorrosion property of TiO_2 . WO_3 can store the electrons generated by TiO_2 under light irradiation [6]. It also can improve the separation of electron-hole pairs, resulting in high anticorrosion capability [10] [11] [15].

Anticorrosion property of the sample was examined by four-point probe to

determine the conductivity of the test specimen. If the conductivity of the specimen is high, the oxidative capacity is high, and its ability of anticorrosion is low. By applying an electric potential (1 V) and current (0.4 A) to the sample, the conductivity was zero in each sample, except the bare 304 stainless steel as shown in **Table 4**, indicating that all samples with coating had high anticorrosion property in the presence of and absence of light illumination.

3.6. Analysis by Cyclic Voltammeter

The corrosion resistance and the behavior of materials were evaluated by the potentiostatic and potentiodynamic polarization methods. **Figure 6** shows that the I-V curves of all samples were very smooth in the range between -0.6 V and -0.05 V. It illustrates that no obvious electrochemical reactions occurred in this region. This result has been initially applied to explain that coating onto the substrate would retard the electrochemical reactions.

Figure 6 shows that WT (4) sample had the lowest current density and TiO_2 sample had the highest current density. High current density infers low anticorrosion property. **Figure 6** shows that the best sample had the weight ratio of TiO_2 : WO_3 of 100:4. The amounts of charge of all samples are listed in **Table 5**. The higher the amount of charge means the lower the anticorrosion capability.

The results show that all of the samples had better anticorrosion capability than the unmodified TiO_2 .

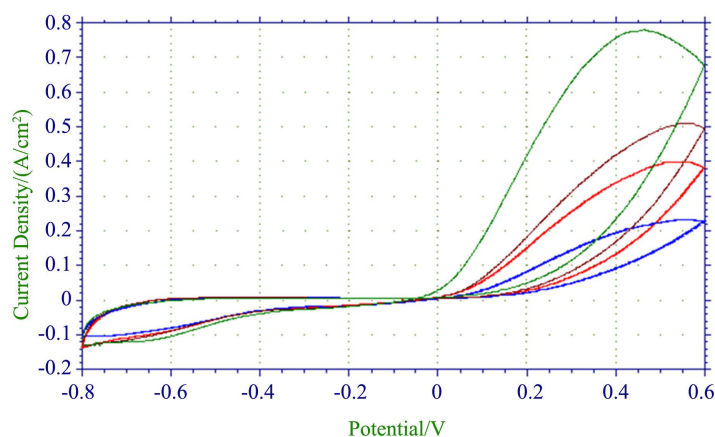


Figure 6. The I-V curve of coated W-modified TiO_2 sol onto type 304 stainless steel. From top to bottom are TiO_2 , WT (1), WT (2), and WT (4).

Table 4. The experimental values of four-point probe for all samples.

Sample	With light irradiation	Without light illumination
Bare 304 stainless steel	1.002 V, 0.260 A	1.002 V, 0.260 A
TiO_2	X	X
WT (0.5)	X	X
WT (1)	X	X
WT (2)	X	X

“X” means that the conductivity was zero.

Table 5. Amount of charge of all samples.

Sample	Q ($10^{-1} \times C$)
TiO ₂	10.47
WT (0.5)	10.08
WT (1)	9.85
WT (2)	8.19
WT (4)	8.13

4. Conclusions

A series of WO₃-modified TiO₂ sols with various WO₃ contents were synthesized by peroxo sol-gel method. The as-prepared WO₃-modified TiO₂ sols were transparent with very light yellow color. The sols were very stable even after 2 years. The sol was used to coat on 304 stainless steel by dip coating for anticorrosion test. Its hardness reached 2 H after drying at 100 °C, and reached 5 H after annealing at 400 °C.

The crystalline phase of TiO₂ in sol was anatase. There were no WO₃ XRD peaks in the WO₃-TiO₂ sols, indicating that WO₃ particles were very small, possibly incorporating into TiO₂ structure, providing the amount of WO₃ was very small. The TiO₂ particles were rhombus shape. WO₃-TiO₂ had smaller size area than pure TiO₂. The SEM results showed that the film coated onto glass substrate were very uniform. The WO₃-TiO₂ coating on 304 stainless steel had better anticorrosion capability than the unmodified TiO₂ coating. The optimum weight ratio of TiO₂: WO₃ was 100:4.

Acknowledgements

This research was supported by the Ministry of Science and Technology, Taiwan.

Conflicts of Interest

The authors declare no conflicts of interest regarding the publication of this paper.

References

- [1] Shan, C.X., Hou, X. and Choy, K.L. (2008) Corrosion Resistance of TiO₂ Films Grown on Stainless Steel by Atomic Layer Deposition. *Surface and Coatings Technology*, **202**, 2399-2402. <https://doi.org/10.1016/j.surfcoat.2007.08.066>
- [2] Yuan, J. and Tsujikawa, S. (1995) Characterization of Sol-Gel-Derived TiO₂ Coatings and Their Photoeffects on Copper Substrates. *Journal of Electrochemical Society*, **142**, 3444-3455. <https://doi.org/10.1149/1.2050002>
<https://citeseerx.ist.psu.edu/viewdoc/download?doi=10.1.1.846.8347&rep=rep1&type=pdf>
- [3] Tatsuma, T., Saitoh, S., Ohko, Y. and Fujishima, A. (2001) TiO₂-WO₃ Photoelectrochemical Anticorrosion System with an Energy Storage Ability. *Chemistry of Materials*, **13**, 2838-2842. <https://doi.org/10.1021/cm010024k>

- [4] Ngaotrakanwivat, P., Tatsuma, T., Saitoh, S., Ohko, Y. and Fujishima, A. (2003) Charge-Discharge Behavior of TiO₂-WO₃ Photocatalysis Systems with Energy Storage Ability. *Physical Chemistry and Chemical Physics*, **5**, 3234-3237. <https://pubs.rsc.org/en/content/articlelanding/2003/cp/b304181f#!divAbstract> <https://doi.org/10.1039/B304181F>
- [5] Kalidindi, N.R., Manciu, F.S. and Ramana, C.V. (2011) Crystal Structure, Phase, and Electrical Conductivity of Nanocrystalline W_{0.95}Ti_{0.05}O₃ Thin Films. *ACS Applied Materials Interfaces*, **3**, 863-868. <https://doi.org/10.1021/am101209d>
- [6] Yang, Y. and Cheng, Y.F. (2020) Visible Light Illuminated High-Performance WO₃-TiO₂-BiVO₄ Nanocomposite Photoanodes Capable of Energy Self-Storage for Photo-Induced Cathodic Protection. *Corrosion Science*, **164**, 108333-108340. <https://www.sciencedirect.com/science/article/abs/pii/S0010938X19317160> <https://doi.org/10.1016/j.corsci.2019.108333>
- [7] Zhao, D., Chen, C., Yu, C., Ma, W. and Zhao, J. (2009) Photoinduced Electron Storage in WO₃/TiO₂ Nanohybrid Material in the Presence of Oxygen and Postirradiated Reduction of Heavy Metal Ions. *Journal Physical Chemistry C*, **113**, 13160-13165. <https://doi.org/10.1021/jp9002774>
- [8] Couselo, N., Einschlag, F.S.G., Candal, R.J. and Jobbágy, M. (2008) Tungsten-Doped TiO₂ vs. Pure TiO₂ Photocatalysts: Effects on Photobleaching Kinetics and Mechanism. *Journal Physical Chemistry C*, **112**, 1094-1100.
- [9] Tatsuma, T., Saitoh, S., Ngaotrakanwivat, P., Ohko, Y. and Fujishima, A. (2002) Energy Storage of TiO₂-WO₃ Photocatalysis Systems in the Gas Phase. *Langmuir*, **18**, 7777-7779. <https://doi.org/10.1021/la026011i>
- [10] Park, H., Kim, K.Y. and Choi, W. (2002) Photoelectrochemical Approach for Metal Corrosion Prevention Using a Semiconductor Photoanode. *Journal Physical Chemistry B*, **106**, 4775-4781. <https://doi.org/10.1021/jp025519r>
- [11] Wang, X., Xu, H., Nan, Y., Sun, X., Duan, J., Huang, Y. and Hou, B. (2020) Research Progress of TiO₂ Photocathodic Protection to Metals in Marine Environment. *Journal of Oceanology and Limnology*, **38**, 1018-1044. https://www.researchgate.net/publication/342848348_Research_progress_of_TiO2_photocathodic_protection_to_metals_in_marine_environment <https://doi.org/10.1007/s00343-020-0110-x>
- [12] Xia, Y., Cheng, H., Duo, L., Zhang, D., Chen, X., Shi, S. and Lei, L. (2020) Anticorrosion Reinforcement of Waterborne Polyacrylate Coating with Nano-TiO₂ Loaded Graphene. *Journal of Applied Polymer Science*, **137**, 48733-48740. <https://doi.org/10.1002/app.48733>
- [13] Krishnan, A., Joseph, B., Bhaskar, K.M., Suma, M.S. and Shibli, S.M.A. (2019) Unfolding the Anticorrosive Characteristics of TiO₂-WO₃ Mixed Oxide Reinforced Polyaniline Composite Coated Mild Steel in Alkaline Environment. *Polymer Composites*, **40**, 2400-2409. <https://doi.org/10.1002/pc.25103>
- [14] Liang, Y., Guan, Z.C., Wang, H.P. and Du, R.G. (2017) Enhanced Photoelectrochemical Anticorrosion Performance of WO₃/TiO₂ Nanotube Composite Films Formed by Anodization and Electrodeposition. *Electrochemistry Communications*, **77**, 120-123. <https://www.sciencedirect.com/science/article/pii/S1388248117300693> <https://doi.org/10.1016/j.elecom.2017.03.008>
- [15] Obstarczyk, A., Mazur, M., Kaczmarek, D., Domaradzki, J., Wojcieszak, D., Grobelny, M. and Kalisz, M. (2020) Influence of Post-process Annealing Temperature on Structural, Optical, Mechanical and Corrosion Properties of Mixed TiO₂-WO₃ Thin Films. *Thin Solid Films*, **698**, e137856. <https://doi.org/10.1016/j.tsf.2020.137856>

- <https://www.sciencedirect.com/science/article/abs/pii/S0040609020300717>
- [16] Ashoka, N.B., Swamy, B.E.K., Jayadevappa, H. and Sharma, S.C. (2020) Simultaneous Electroanalysis of Dopamine, Paracetamol and Folic Acid Using TiO₂-WO₃ Nanoparticle Modified Carbon Paste Electrode. *Journal of Electroanalytical Chemistry*, **859**, e113819. <https://doi.org/10.1016/j.jelechem.2020.113819>
<https://www.sciencedirect.com/science/article/abs/pii/S1572665720300023>
- [17] Abdeen, D.H., Hachach, M.E., Koc, M. and Atieh, M.A. (2019) A Review on the Corrosion Behaviour of Nanocoatings on Metallic Substrates. *Materials*, **12**, 210. <https://pubmed.ncbi.nlm.nih.gov/30634551/>
<https://doi.org/10.3390/ma12020210>
- [18] Sasirekha, N., Rajesh, B. and Chen, Y.W. (2009) Synthesis of TiO₂ Sol in a Neutral Solution Using TiCl₄ as a Precursor and H₂O₂ as an Oxidizing Agent. *Thin Solid Films*, **518**, 43-48. <https://doi.org/10.1016/j.tsf.2009.06.015>
<https://www.sciencedirect.com/science/article/abs/pii/S0040609009010554>
- [19] Tryba, B., Piszcz, M. and Morawsk, A.W. (2009) Photocatalytic Activity of TiO₂-WO₃ Composites. *International Journal of Photoenergy*, **2009**, Article ID: 297319. <https://doi.org/10.1155/2009/297319>
[https://www.researchgate.net/publication/26844164_Photocatalytic_Activity_of_TiO₂-WO₃_Composites](https://www.researchgate.net/publication/26844164_Photocatalytic_Activity_of_TiO2-WO3_Composites)